

# EL-MLFFs: Ensemble Learning of Machine Learning Force Fields

Bangchen Yin<sup>1\*</sup>, Yue Yin<sup>1†</sup>, Yuda W. Tang<sup>1</sup>, and Hai Xiao<sup>‡1</sup>

<sup>1</sup>Department of Chemistry, Tsinghua University, Beijing 100084, China

March 27, 2024

## Abstract

Machine learning force fields (MLFFs) have emerged as a promising approach to bridge the accuracy of quantum mechanical methods and the efficiency of classical force fields. However, the abundance of MLFF models and the challenge of accurately predicting atomic forces pose significant obstacles in their practical application. In this paper, we propose a novel ensemble learning framework, EL-MLFFs, which leverages the stacking method to integrate predictions from diverse MLFFs and enhance force prediction accuracy. By constructing a graph representation of molecular structures and employing a graph neural network (GNN) as the meta-model, EL-MLFFs effectively captures atomic interactions and refines force predictions. We evaluate our approach on two distinct datasets: methane molecules and methanol adsorbed on a Cu(100) surface. The results demonstrate that EL-MLFFs significantly improves force prediction accuracy compared to individual MLFFs, with the ensemble of all eight models yielding the best performance. Moreover, our ablation study highlights the crucial roles of the residual network and graph attention layers in the model’s architecture. The EL-MLFFs framework offers a promising solution to the challenges of model selection and force prediction accuracy in MLFFs, paving the way for more reliable and efficient molecular simulations.

## 1 Introduction

In the complex world of computational simulations, the synergy between potential energy surfaces (PES) and force fields is fundamental to unlocking the dynamics of molecular systems [Babin et al.(2013)Babin, Leforestier, Jiang and Guo(2013), Zhang et al.(2019)Zhang, Lin, Wang, Car, and E, Habershon et al.(2013)Habershon, Manolopoulos]. Force fields, which capture the potential energies arising from atomic interactions, work in harmony with PES to propel simulations across a range of scientific fields. This union between force fields and PES is crucial for accurately depicting molecular behaviors, thereby enriching simulations of chemical reactions, molecular dynamics, and the properties of materials [Zheng et al.(2019)Zheng, Chu, Zhao, Zhang, Guo, Wang, J Vidal-Limon et al.(2022)Vidal-Limon, Aguilar-Toala, and Liceaga, Ariga et al.(2016)Ariga, Li, Fei, Ji, and Hill]. In particular, force fields calibrate the potential energy surface, orchestrating the movements of atoms and molecules. With the progression of computational techniques that include quantum mechanics and machine learning, the collaboration between force fields and PES achieves heightened precision and efficiency.

In the domain of molecular simulations, traditional force fields, anchored in empirical formulas, have been preferred for their computational speed and straightforwardness [Cornell et al.(1995)Cornell, Cieplak, Bayly, Gould, Brooks et al.(2009)Brooks, Brooks, Mackerell, Nilsson, Petrella, Roux, Won, Archontis, Bartels, Boresch, Caffisch, Caves DAW and BASKES(1984), Jorgensen et al.(1996)Jorgensen, Maxwell, and TiradoRives, RAPPE et al.(1992)RAPPE, CA Scott et al.(1999)Scott, Hünenberger, Tironi, Mark, Billeter, Fennen, Torda, Huber, Krüger, and van Gunsteren]. Derived from experimental observations, these force fields are adept at mimicking bulk properties and

\*These authors contributed equally to this work.

†These authors contributed equally to this work.

‡Corresponding author. Email: haixiao@tsinghua.edu.cn

straightforward molecular interactions. Yet, their empirical foundation presents challenges in navigating the complex demands of elaborate molecular systems, especially when dealing with nuanced quantum mechanical effects and dynamic processes.

While traditional force fields are effective in situations where computational speed is paramount, they face limitations in accurately simulating the vast array of molecular environments. The advent of machine learning force fields [Durumeric et al.(2023)Durumeric, Charron, Templeton, Musil, Bonneau, Pasos-Trejo, Chen, Jinnouchi et al.(2019a)Jinnouchi, Karsai, and Kresse, Chmiela et al.(2023)Chmiela, Vassilev-Galindo, Unke, Kabylda, Sa marks a significant evolution in simulation strategies. By tapping into large datasets, these innovative models overcome the limitations inherent in empirical force fields, providing a more versatile and adaptive solution. Machine learning force fields endeavor to achieve an optimal balance by capturing the precision of quantum mechanical approaches while maintaining the computational efficiency characteristic of traditional force fields [Chmiela et al.(2018)Chmiela, Saucedo, Mueller, and Tkatchenko, Jinnouchi et al.(2019b)Jinnouchi, Lahnsteiner, Karsai, Kresse, and Bokdam, Dral(2020), Botu et al.(2017)Botu, Batra, C

This investigation explores the strengths and limitations of traditional force fields and empirical models, shedding light on their benefits and challenges. As we traverse the molecular landscape, the advent of machine learning force fields stands out as a groundbreaking development, poised to transform our capacity to simulate and understand the complexities of varied molecular systems. The intricate balance between traditional methods and innovative approaches is crucial for enhancing the precision and relevance of molecular simulations in the dynamic world of scientific research and technological advancements.

Within the sphere of machine learning force fields, a variety of methodologies have surfaced, each offering distinct advantages to the arsenal of simulation tools. Gaussian Approximation Potentials (GAP) utilize Gaussian processes [Bartók et al.(2010)Bartók, Payne, Kondor, and Csányi, Deringer and Csányi(2017), Deringer et al.(2018)Deringer, Pickard, and Csányi, Rowe et al.(2020)Rowe, Deringer, Gasparotto, Csányi, and Michaelid excelling at capturing the subtle quantum mechanical phenomena across different molecular systems. Artificial Neural Networks (ANNs) bring flexibility in deciphering complex patterns [Behler and Parrinello(2007), Smith et al.(2017)Smith, Isayev, and Roitberg], whereas Deep Neural Networks (DNNs) [Zhang et al.(2018)Zhang, Han, W Behler(2016)] and Graph Neural Networks (GNNs) [Schütt et al.(2017)Schütt, Kindermans, Saucedo, Chmiela, Tkatchenko, Gilmer et al.(2017)Gilmer, Schoenholz, Riley, Vinyals, and Dahl] expand these capabilities, achieving superior accuracy in depicting potential energy landscapes. Moreover, the integration of the Transformers architecture [Liao et al.(2023)Liao, Wood, Das, and Smidt] demonstrates remarkable adaptability, particularly adept at modeling long-range interactions within molecular frameworks.

Researchers, leveraging their extensive experience, have adeptly applied these machine learning force field models to tangible systems, shedding light on reaction mechanisms and material property predictions [Podryabinkin et al.(2019)Podryabinkin, Tikhonov, Shapeev, and Oganov]. This amassed knowledge sets the stage for further progress in simulating and understanding the intricate molecular landscapes.

Although machine learning force fields show remarkable prowess in energy prediction, attaining similar levels of accuracy in force prediction presents a notable challenge. This gap diminishes their utility in applications demanding precise force calculations [Henkelman et al.(2000)Henkelman, Uberuaga, and Jónsson]. Furthermore, the wide spectrum of models available, from Gaussian processes to sophisticated neural network designs, complicates the task of selecting the most fitting model for particular molecular simulations. Addressing these obstacles is essential for improving the precision and practicality of machine learning force fields in detailing complex molecular phenomena.

Ensemble learning techniques, such as Bagging, Boosting, and Stacking [Breiman(1996), Freund and Schapire(1995), Fernández-Delgado et al.(2014)Fernández-Delgado, Cernadas, Barro, and Amorim, Wolpert(1992), Freund and Schapire(1 could offer viable solutions to these challenges within machine learning force fields. Bagging, which employs multiple models trained on various dataset segments, might reduce overfitting and boost overall stability, thereby enriching the portrayal of potential energy landscapes. On the other hand, Boosting focuses on incrementally improving weak learners, potentially enhancing force prediction accuracy by concentrating on areas of difficulty. By increasing the emphasis on incorrectly predicted instances, Boosting aims to offset the inherent limitations of individual models. Stacking, which consolidates diverse models and their predictions through a meta-model, suggests a strategy to amalgamate strengths and tackle the issue of model selection. In the context of machine learning force fields, ensemble learning represents an exploratory yet promising direction to heighten accuracy and resilience, possibly charting a course to surmount existing barriers and elevate the precision and relevance of molecular

simulations.

This paper delves into the prospective application of the Stacking method in machine learning force fields. Stacking, by amalgamating predictions from various models via a meta-model, is poised to address the challenges tied to force prediction accuracy and model selection intricacies. By harmonizing insights across different machine learning models, Stacking could provide a refined approach for depicting the complexities of potential energy surfaces and force dynamics in molecular systems. Although the practical efficacy of this application is yet to be confirmed, exploring Stacking within machine learning force fields paves new paths for augmenting accuracy and durability, potentially fostering significant strides in the precision and utility of molecular simulations.

## 2 Method

### 2.1 Stacking

Stacked generalization, or *stacking*, employs multiple base models and a meta-model to enhance predictive accuracy. The methodology unfolds across two primary stages:

**Stage 1: Base Model Predictions.** Given a dataset

$$D = \{(x_i, y_i)\}_{i=1}^N, \tag{1}$$

where  $x_i$  represents the feature vector and  $y_i$  the corresponding target, a collection of  $M$  base models  $\{f_m\}_{m=1}^M$  is trained. Each base model  $f_m : \mathbb{R}^d \rightarrow \mathbb{R}$  (for regression) or  $f_m : \mathbb{R}^d \rightarrow \{c_1, c_2, \dots, c_k\}$  (for classification) generates a prediction  $\hat{y}_{i,m} = f_m(x_i)$  for each instance  $x_i$ .

**Stage 2: Meta-Model Integration.** The predictions from the base models are aggregated into a new feature vector for each instance,

$$\tilde{x}_i = [\hat{y}_{i,1}, \hat{y}_{i,2}, \dots, \hat{y}_{i,M}], \tag{2}$$

resulting in a transformed dataset  $\tilde{D} = \{(\tilde{x}_i, y_i)\}_{i=1}^N$ . A meta-model  $g : \mathbb{R}^M \rightarrow \mathbb{R}$  (for regression) or  $g : \mathbb{R}^M \rightarrow \{c_1, c_2, \dots, c_k\}$  (for classification) is subsequently trained on  $\tilde{D}$  to predict the target  $y$  based on the meta-features  $\tilde{x}$ .

The objective of stacking is formalized as minimizing the loss function

$$L(y, g(\tilde{x})), \tag{3}$$

where  $L$  quantifies the difference between the actual targets  $y$  and the predictions made by the meta-model  $g$  on the aggregated predictions  $\tilde{x}$  from the base models. This technique leverages the diversity in the base models’ predictions, enabling the meta-model to discern a more intricate mapping from the feature space to the target space, thereby potentially exceeding the predictive capabilities of any single base model.

This ensemble technique is particularly effective when base models exhibit complementary predictive behaviors, allowing the meta-model to capture complex patterns in the data that might be overlooked by individual models. Through this collaborative predictive framework, stacking provides a robust mechanism for attaining superior performance in diverse predictive tasks.

### 2.2 Our Structure

Within our methodology, we consider a dataset  $D = \{(x_i, y_i)\}_{i=1}^N$ , where each  $x_i$  encapsulates the input features of a molecular structure, and  $y_i \in \mathbb{R}^d$  represents the corresponding true atomic forces, with  $d$  being the dimensionality of the force vector for each atom.

We deploy a set of  $M$  machine learning force fields, denoted as  $\{f_m\}_{m=1}^M$ , each trained on  $D$ . For a given molecular structure represented by  $x_i$ , the predicted force by the  $m$ -th model on the  $j$ -th atom is  $\hat{y}_{ij}^m = f_m(x_i[j])$ , where  $x_i[j]$  indicates the feature vector of the  $j$ -th atom in the  $i$ -th molecular structure.

To construct a graph representation  $G_i = (V_i, E_i)$  for each molecular structure  $x_i$ , we define  $V_i$  as the set of nodes (atoms) and  $E_i$  as the set of edges (bonds). The feature vector for each node (atom)  $j$  in graph  $G_i$  is formulated as:

$$v_{ij} = [\hat{y}_{ij}^1, \hat{y}_{ij}^2, \dots, \hat{y}_{ij}^M, \text{atomic type}_{ij}],$$

where the inclusion of atomic type $_{ij}$  integrates atomic type information into the node features.

A Graph Neural Network (GNN) is trained to minimize the Mean Squared Error (MSE) between its predicted forces  $\hat{y}_i^{\text{GNN}}$  and the true forces  $y_i$  across all atoms in all structures within the dataset. The MSE objective function is defined as:

$$\text{Objective Function: } \min_{\theta} \frac{1}{N} \sum_{i=1}^N \sum_{j=1}^{d_i} (\hat{y}_{ij}^{\text{GNN}}(\theta, v_{ij}) - y_{ij})^2,$$

where  $\theta$  represents the parameters of the GNN,  $d_i$  is the number of atoms in the  $i$ -th structure,  $v_{ij}$  is the feature vector of the  $j$ -th atom in the  $i$ -th structure, and  $\hat{y}_{ij}^{\text{GNN}}(\theta, v_{ij})$  denotes the force predicted by the GNN for the  $j$ -th atom in the  $i$ -th structure.

This concise and mathematical formulation captures the essence of our method, emphasizing the integration of predictions from diverse machine learning force fields and the utilization of a GNN to refine the prediction of atomic forces within molecular systems.

### 2.3 Graph Representation

In our methodology, we construct a graph representation for molecular structures to model interactions between atoms effectively. This involves several mathematical operations and transformations, outlined as follows:

**1. Atom Type Encoding:** Each atom type within a set  $\{a_1, a_2, \dots, a_n\}$  is mapped to a unique integer identifier, resulting in a mapping  $\{t_1, t_2, \dots, t_n\}$  where  $t_i$  corresponds to the unique identifier for atom type  $a_i$ . The mapping function is defined as:

$$f(a_i) = t_i.$$

**2. Fractional to Cartesian Coordinates Transformation:** The transformation from fractional coordinates  $\mathbf{f}$  to Cartesian coordinates  $\mathbf{c}$ , relative to the lattice vectors of the unit cell, is given by:

$$\mathbf{c} = \mathbf{f} \cdot \mathbf{L},$$

where  $\mathbf{L}$  denotes the matrix of lattice vectors.

**3. Cartesian to Fractional Coordinates Transformation:** The inverse transformation from Cartesian coordinates  $\mathbf{c}$  to fractional coordinates  $\mathbf{f}$  is achieved using the inverse lattice vectors matrix  $\mathbf{L}^{-1}$ :

$$\mathbf{f} = \mathbf{c} \cdot \mathbf{L}^{-1}.$$

**4. Periodic Boundary Conditions Distance Calculation:** To account for periodic boundary conditions, the difference in fractional coordinates  $\Delta\mathbf{f}_{ij}$ , adjusted for periodicity, is:

$$\Delta\mathbf{f}_{ij} = \mathbf{f}_i - \mathbf{f}_j - \text{round}(\mathbf{f}_i - \mathbf{f}_j).$$

The Cartesian distance  $\Delta\mathbf{c}_{ij}$  is then obtained by converting  $\Delta\mathbf{f}_{ij}$  back to Cartesian coordinates and computing the Euclidean distance.

**5. Edge Index and Attributes Construction:** The graph is constructed by identifying pairs of atoms  $(i, j)$  within a cutoff distance  $d_{\text{cutoff}}$  and ensuring  $i \neq j$ . The edge indices and attributes (distances  $d_{ij}$ ) are determined based on:

$$d_{ij} < d_{\text{cutoff}}, \quad i \neq j.$$

This approach captures the connectivity and spatial relationships between atoms, crucial for the graph-based representation.

By following these steps, a graph data object is created, encapsulating atomic features, edge indices, edge attributes, and target forces. This representation allows for the application of graph neural networks (GNNs) to learn from complex atomic interaction patterns, aiming for accurate force prediction in the molecular system.

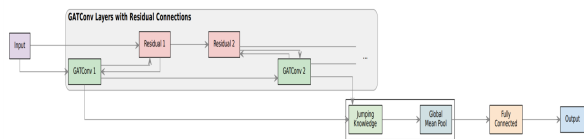


Figure 1: Model Architecture

## 2.4 Model Architecture

The `GNNModel` is architected to process graphs representing molecular structures, where nodes correspond to atoms, characterized by their atomic types and predicted forces, and edges represent atomic interactions. The architecture unfolds as follows 1:

**1. Graph Attention Layers:** At the heart of the `GNNModel` lies a sequence of eight GAT convolutional layers [Veličković et al.(2018)Veličković, Cucurull, Casanova, Romero, Liò, and Bengio] that iteratively refine node features through attention-based aggregation. The formulation for the operation performed by the  $k$ -th GATConv layer is given by:

$$x^{(k+1)} = \text{ReLU} \left( \text{GATConv}^{(k)}(x^{(k)}, \text{edge\_index}; \Theta^{(k)}) + \text{Res}^{(k)}(x^{(k)}), \right) \quad (4)$$

where  $x^{(k)}$  represents the node features at the  $k$ -th layer,  $\text{GATConv}^{(k)}$  denotes the GAT convolution operation with parameters  $\Theta^{(k)}$ , and  $\text{Res}^{(k)}$  indicates the residual connection [He et al.(2015)He, Zhang, Ren, and Sun] at the  $k$ -th layer.

**2. Jumping Knowledge Integration:** Following the attention layers, a Jumping Knowledge (JK) mechanism integrates [Xu et al.(2018)Xu, Li, Tian, Sonobe, ichi Kawarabayashi, and Jegelka] outputs across all layers to encapsulate both local and global structural insights:

$$x_{jk} = \text{JK}([x^{(1)}, x^{(2)}, \dots, x^{(8)}]), \quad (5)$$

where  $x_{jk}$  denotes the concatenated feature vector from all GATConv layers.

**3. Pooling and Output:** The architecture concludes with a global mean pooling [Goodfellow et al.(2016)Goodfellow, operation, aggregating node features across the graph, followed by a fully connected layer that maps the pooled representation to the predicted atomic forces:

$$x_{out} = \text{FC}(\text{GlobalMeanPool}(x_{jk}); \Phi). \quad (6)$$

Here, FC signifies the fully connected layer with parameters  $\Phi$ , transforming the aggregated graph features to the output dimensionality aligned with the target forces for each atom in the molecular structure.

Through its integration of graph attention layers, multi-head attention, and residual connections, the `GNNModel` offers a robust framework for understanding and predicting forces within molecular systems, highlighting the potential of advanced GNN architectures in the realm of molecular dynamics predictions.

## 2.5 Data

In this study, we utilized two distinct datasets as the focal points of our investigation. The first dataset comprises relatively straightforward data on single methane molecules, which contains 5000 training frames and 500 test frames. The second dataset encompasses data related to methanol molecules adsorbed on the Cu(100) surface. Specifically, the methanol adsorption dataset consists of 8,102 training instances and 500 test instances. This system is characterized by a three-layer Cu(4x4) (100) surface, atop which numerous conformations of methanol molecules are presented.

All data were generated using the Vienna *Ab initio* Simulation Package (VASP) [Kresse and Furthmüller(1996)], with the VASPKit code [Wang et al.(2021)Wang, Xu, Liu, Tang, and Geng] employed for post-processing the computed data. The exchange-correlation energy was addressed using the Generalized Gradient Approximation (GGA) [Perdew et al.(1996)Perdew, Burke, and Ernzerhof] alongside the Perdew-Burke-Ernzerhof functional. The interaction between core and valence electrons was delineated using

the Projected Augmented Wave (PAW) basis set [Kresse and Joubert(1999)]. For the simulation parameters, we specified `KSPACING=0.5` in the `INCAR` file, and the Gamma point was omitted from the k-space sampling. An energy cutoff of 400 eV was established to ensure computational accuracy and efficiency.

## 2.6 Machine Learning Force Fields

In our experimental setup, we meticulously selected and deployed a diverse ensemble of eight models derived from four innovative types of machine learning force fields. The allocation and specifics of these models are as follows:

1. **DeepMD Model:** This category encompasses three distinct models, each tailored to a unique descriptor:
  - `se_e2_a`
  - `se_e2_r`
  - `se_e3`

These three models are denoted as **dp1**, **dp2**, and **dp3**, respectively.

2. **SchNet Model:** Under the SchNet framework, we investigated three models, each differentiated by the number of basis functions (`n_basis`), thus constituting three models. These three models are denoted as **sch1**, **sch2**, and **sch3**, respectively.
3. **PaiNN:** We integrated one model from the PaiNN force field, renowned for its ability to capture the quantum-mechanical nature of atomic interactions. This model is denoted as **painn**.
4. **NEP:** Additionally, a single model from the NEP force field was employed, bringing a unique perspective to our model ensemble. This model is denoted as **nep**.

This carefully curated collection of models from DeepMD, SchNet, PaiNN, and NEP force fields provides a comprehensive toolkit, enabling a broad and nuanced exploration of molecular dynamics predictions.

## 2.7 Metrics

We use Root Mean Square Error (RMSE) as a metric to describe the precision of MLFFs and our method:

$$\overline{\text{RMSE}} = \frac{1}{m} \sum_{j=1}^m \sqrt{\frac{1}{n_j} \sum_{i=1}^{n_j} (y_{ij} - \hat{y}_{ij})^2} \quad (7)$$

$m$  is the number of systems;  $n_j$  is the number of data points for the  $j^{\text{th}}$  system;  $y^{ij}$  is the observed value at the  $i^{\text{th}}$  data point of the  $j^{\text{th}}$  system;  $\hat{y}_{ij}$  is the predicted value at the  $i^{\text{th}}$  data point of the  $j^{\text{th}}$  system.

# 3 Results

## 3.1 RMSE from MLFFs

To demonstrate the effectiveness of our approach, we first evaluated the Root Mean Square Error (RMSE) of the individual machine learning force fields themselves:

Table 1 presents the RMSE values of 8 machine learning force fields (MLFFs) on two datasets: methane and methanol 2.5. For the simpler methane dataset, only 3 models (dp1, dp2, and dp3) were trained, while for the more complex methanol system, all 8 models were employed. It is important to note that these results do not directly reflect the inherent capabilities of the different MLFFs, as the training details can significantly impact their performance. Further information regarding the training procedures and hyperparameters for each model will be provided in the Appendix.

Table 1: RMSE values for different MLFFs

Models	Methane RMSE(eV/Å)	Methanol RMSE(eV/Å)
dp1	0.0083	0.1027
dp2	0.0446	0.2531
dp3	0.0092	0.0841
sch1	–	0.1336
sch2	–	0.1862
sch3	–	0.1343
nep	–	0.0632
painn	–	0.0361

### 3.2 RMSE from our method

Our proposed method was trained and evaluated on the two datasets mentioned in the previous section, yielding the following results:

Table 2: RMSE values for Methane Dataset

Models	RMSE(eV/Å)
dp1	0.0009
dp2	0.0008
dp3	0.0008
dp1, dp2	0.0008
dp1, dp3	0.0007
dp2, dp3	0.0007
dp1, dp2, dp3	0.0008

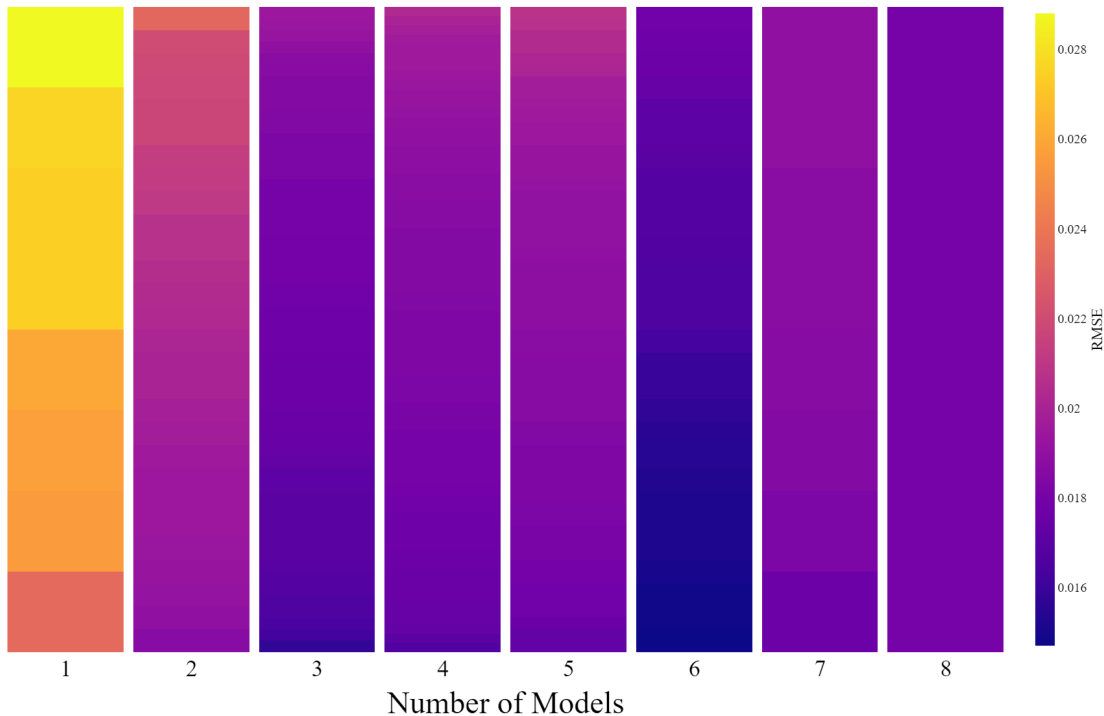


Figure 2: RMSE values of Methanol

Table 2 presents the test performance of the 3 DeepMD models on the methane dataset, from which 7 ensembles were constructed through various combinations. Overall, the results demonstrate an order of magnitude improvement relative to the original machine learning force field models. Additionally, a marginal enhancement in performance is observed as the number of models in the ensemble increases. In the Figure 2, the refined insights drawn from our ensemble analysis are visually depicted through a comprehensive heat-map, meticulously evaluating performance fluctuations across diverse model combinations within the ensemble framework, encompassing all possible subsets from the eight selected models. This heat-map acts as a bridge between raw performance data and our analytical conclusions, highlighting the critical balance required between the number of models employed and the actual efficiency achieved. This aligns with our overarching narrative by identifying a threshold in model integration, beyond which additional models do not lead to proportional increases in predictive accuracy, and instead approach redundancy. Our methodology is not merely about augmenting numbers for diversity’s sake but aims to cultivate optimal synergy that transcends traditional modeling approaches, thereby ensuring computational pragmatism while enhancing the predictive capabilities of the ensemble framework.

The results demonstrate that our models are indeed capable of effectively capturing and synthesizing information from various machine learning force fields (MLFFs), enabling them to generate superior predictions through analysis and ensemble techniques. It is noteworthy that owing to the simplicity of our model architecture, our proposed method is computationally inexpensive and efficient. Consequently, our approach opens up a novel avenue in the realm of machine learning force fields, with potential applications extending to diverse tasks such as property prediction and material design.

Furthermore, our method could provide a valuable and reliable solution to the current challenge faced by users, where the abundance of high-quality MLFFs available renders the selection process increasingly intricate. By harnessing the strengths of multiple MLFFs through ensemble modeling, our technique mitigates the need for a priori selection, thereby offering a more comprehensive and robust approach to leverage the collective predictive power of these force fields.

In essence, our work not only introduces an innovative methodology for enhancing the predictive capabilities of MLFFs but also presents a viable solution to the growing complexity of model selection, underscoring its significance and potential impact in the field of computational materials science.

## Code and data availability

Codes and data are provided in <https://github.com/zmyybc/EL-MLFFs/tree/master>.

## References

- [Ariga et al.(2016)Ariga, Li, Fei, Ji, and Hill] Katsuhiko Ariga, Junbai Li, Jinbo Fei, Qingmin Ji, and Jonathan P. Hill. 2016. [Nanoarchitectonics for dynamic functional materials from atomic-/molecular-level manipulation to macroscopic action](#). *ADVANCED MATERIALS*, 28(6):1251–1286.
- [Babin et al.(2013)Babin, Leforestier, and Paesani] Volodymyr Babin, Claude Leforestier, and Francesco Paesani. 2013. [Development of a “first principles” water potential with flexible monomers: Dimer potential energy surface, vrt spectrum, and second virial coefficient](#). *JOURNAL OF CHEMICAL THEORY AND COMPUTATION*, 9(12):5395–5403.
- [Bartók et al.(2010)Bartók, Payne, Kondor, and Csányi] Albert P. Bartók, Mike C. Payne, Risi Kondor, and Gábor Csányi. 2010. [Gaussian approximation potentials: The accuracy of quantum mechanics, without the electrons](#). *Phys. Rev. Lett.*, 104:136403.
- [Behler and Parrinello(2007)] Jörg Behler and Michele Parrinello. 2007. [Generalized neural-network representation of high-dimensional potential-energy surfaces](#). *Phys. Rev. Lett.*, 98:146401.
- [Behler(2016)] Jörg Behler. 2016. [Perspective: Machine learning potentials for atomistic simulations](#). *The Journal of Chemical Physics*, 145(17):170901.

- [Botu et al.(2017)Botu, Batra, Chapman, and Ramprasad] V. Botu, R. Batra, J. Chapman, and R. Ramprasad. 2017. [Machine learning force fields: Construction, validation, and outlook](#). *JOURNAL OF PHYSICAL CHEMISTRY C*, 121(1):511–522.
- [Breiman(1996)] Leo Breiman. 1996. [Bagging predictors](#). *Machine Learning*, 24:123–140.
- [Brooks et al.(2009)Brooks, Brooks, Mackerell, Nilsson, Petrella, Roux, Won, Archontis, Bartels, Boresch, Caffisch, Caves, B. R. Brooks, C. L. Brooks, III, A. D. Mackerell, Jr., L. Nilsson, R. J. Petrella, B. Roux, Y. Won, G. Archontis, C. Bartels, S. Boresch, A. Caffisch, L. Caves, Q. Cui, A. R. Dinner, M. Feig, S. Fischer, J. Gao, M. Hodoscek, W. Im, K. Kuczera, T. Lazaridis, J. Ma, V. Ovchinnikov, E. Paci, R. W. Pastor, C. B. Post, J. Z. Pu, M. Schaefer, B. Tidor, R. M. Venable, H. L. Woodcock, X. Wu, W. Yang, D. M. York, and M. Karplus. 2009. [Charmm: The biomolecular simulation program](#). *JOURNAL OF COMPUTATIONAL CHEMISTRY*, 30(10, SI):1545–1614.
- [Chmiela et al.(2018)Chmiela, Sauceda, Mueller, and Tkatchenko] Stefan Chmiela, Huziel E. Sauceda, Klaus-Robert Mueller, and Alexandre Tkatchenko. 2018. [Towards exact molecular dynamics simulations with machine-learned force fields](#). *NATURE COMMUNICATIONS*, 9.
- [Chmiela et al.(2023)Chmiela, Vassilev-Galindo, Unke, Kabylda, Sauceda, Tkatchenko, and Mueller] Stefan Chmiela, Valentin Vassilev-Galindo, Oliver T. Unke, Adil Kabylda, Huziel E. Sauceda, Alexandre Tkatchenko, and Klaus-Robert Mueller. 2023. [Accurate global machine learning force fields for molecules with hundreds of atoms](#). *SCIENCE ADVANCES*, 9(2).
- [Cornell et al.(1995)Cornell, Cieplak, Bayly, Gould, Merz, Ferguson, Spellmeyer, Fox, Caldwell, and Kollman] W. D. Cornell, Piotr Cieplak, Christopher I. Bayly, Ian R. Gould, Jr. Merz, Kenneth M., David M. Ferguson, David C. Spellmeyer, Thomas Fox, James W. Caldwell, and Peter A. Kollman. 1995. A second generation force field for the simulation of proteins, nucleic acids, and organic molecules. *Journal of the American Chemical Society*, 117(19):5179–5197.
- [DAW and BASKES(1984)] MS DAW and MI BASKES. 1984. [Embedded-atom method - derivation and application to impurities, surfaces, and other defects in metals](#). *PHYSICAL REVIEW B*, 29(12):6443–6453.
- [Deringer and Csányi(2017)] Volker L. Deringer and Gábor Csányi. 2017. [Machine learning based interatomic potential for amorphous carbon](#). *Phys. Rev. B*, 95:094203.
- [Deringer et al.(2018)Deringer, Pickard, and Csányi] Volker L. Deringer, Chris J. Pickard, and Gábor Csányi. 2018. [Data-driven learning of total and local energies in elemental boron](#). *Phys. Rev. Lett.*, 120:156001.
- [Dral(2020)] Pavlo O. Dral. 2020. [Quantum chemistry in the age of machine learning](#). *JOURNAL OF PHYSICAL CHEMISTRY LETTERS*, 11(6):2336–2347.
- [Durumeric et al.(2023)Durumeric, Charron, Templeton, Musil, Bonneau, Pasos-Trejo, Chen, Kelkar, Noe, and Clementi] Aleksander E. P. Durumeric, Nicholas E. Charron, Clark Templeton, Felix Musil, Klara Bonneau, Aldo S. Pasos-Trejo, Yaoyi Chen, Atharva Kelkar, Frank Noe, and Cecilia Clementi. 2023. [Machine learned coarse-grained protein force-fields: Are we there yet?](#) *CURRENT OPINION IN STRUCTURAL BIOLOGY*, 79.
- [Fernández-Delgado et al.(2014)Fernández-Delgado, Cernadas, Barro, and Amorim] Manuel Fernández-Delgado, Eva Cernadas, Senén Barro, and Dinani Amorim. 2014. Do we need hundreds of classifiers to solve real world classification problems? *J. Mach. Learn. Res.*, 15(1):3133–3181.
- [Freund and Schapire(1995)] Yoav Freund and Robert E. Schapire. 1995. A decision-theoretic generalization of on-line learning and an application to boosting. In *Computational Learning Theory*, pages 23–37, Berlin, Heidelberg. Springer Berlin Heidelberg.
- [Gilmer et al.(2017)Gilmer, Schoenholz, Riley, Vinyals, and Dahl] Justin Gilmer, Samuel S. Schoenholz, Patrick F. Riley, Oriol Vinyals, and George E. Dahl. 2017. [Neural message passing for quantum chemistry](#).

- [Goodfellow et al.(2016)Goodfellow, Bengio, and Courville] Ian Goodfellow, Yoshua Bengio, and Aaron Courville. 2016. *Deep Learning*, volume 1. MIT Press, Cambridge, MA.
- [Habershon et al.(2013)Habershon, Manolopoulos, Markland, and Miller] Scott Habershon, David E. Manolopoulos, Thomas E. Markland, and Thomas F. Miller. 2013. [Ring-polymer molecular dynamics: Quantum effects in chemical dynamics from classical trajectories in an extended phase space](#). *Annual Review of Physical Chemistry*, 64(1):387–413. PMID: 23298242.
- [He et al.(2015)He, Zhang, Ren, and Sun] Kaiming He, Xiangyu Zhang, Shaoqing Ren, and Jian Sun. 2015. [Deep residual learning for image recognition](#).
- [Henkelman et al.(2000)Henkelman, Uberuaga, and Jónsson] Graeme Henkelman, Blas P. Uberuaga, and Hannes Jónsson. 2000. [A climbing image nudged elastic band method for finding saddle points and minimum energy paths](#). *The Journal of Chemical Physics*, 113(22):9901–9904.
- [Jiang and Guo(2013)] Bin Jiang and Hua Guo. 2013. [Permutation invariant polynomial neural network approach to fitting potential energy surfaces](#). *JOURNAL OF CHEMICAL PHYSICS*, 139(5).
- [Jinnouchi et al.(2019a)Jinnouchi, Karsai, and Kresse] Ryosuke Jinnouchi, Ferenc Karsai, and Georg Kresse. 2019a. [On-the-fly machine learning force field generation: Application to melting points](#). *PHYSICAL REVIEW B*, 100(1).
- [Jinnouchi et al.(2019b)Jinnouchi, Lahnsteiner, Karsai, Kresse, and Bokdam] Ryosuke Jinnouchi, Jonathan Lahnsteiner, Ferenc Karsai, Georg Kresse, and Menno Bokdam. 2019b. [Phase transitions of hybrid perovskites simulated by machine-learning force fields trained on the fly with bayesian inference](#). *PHYSICAL REVIEW LETTERS*, 122(22).
- [Jorgensen et al.(1996)Jorgensen, Maxwell, and TiradoRives] WL Jorgensen, DS Maxwell, and J TiradoRives. 1996. [Development and testing of the opls all-atom force field on conformational energetics and properties of organic liquids](#). *JOURNAL OF THE AMERICAN CHEMICAL SOCIETY*, 118(45):11225–11236.
- [Kresse and Furthmüller(1996)] G. Kresse and J. Furthmüller. 1996. Efficient iterative schemes for ab initio total-energy calculations using a plane-wave basis set. *Physical Review B*, 54:11169.
- [Kresse and Joubert(1999)] G. Kresse and D. Joubert. 1999. From ultrasoft pseudopotentials to the projector augmented-wave method. *Physical Review B*, 59:1758.
- [Liao et al.(2023)Liao, Wood, Das, and Smidt] Yi-Lun Liao, Brandon Wood, Abhishek Das, and Tess Smidt. 2023. [Equiformerv2: Improved equivariant transformer for scaling to higher-degree representations](#).
- [Loshchilov and Hutter(2016)] Ilya Loshchilov and Frank Hutter. 2016. Sgdr: Stochastic gradient descent with warm restarts. *arXiv preprint arXiv:1608.03983*.
- [Perdew et al.(1996)Perdew, Burke, and Ernzerhof] J. P. Perdew, K. Burke, and M. Ernzerhof. 1996. Generalized gradient approximation made simple. *Physical Review Letters*, 77:3865.
- [Podryabinkin et al.(2019)Podryabinkin, Tikhonov, Shapeev, and Oganov] Evgeny V. Podryabinkin, Evgeny V. Tikhonov, Alexander V. Shapeev, and Artem R. Oganov. 2019. [Accelerating crystal structure prediction by machine-learning interatomic potentials with active learning](#). *Phys. Rev. B*, 99:064114.
- [RAPPE et al.(1992)RAPPE, CASEWIT, COLWELL, GODDARD, and SKIFF] AK RAPPE, CJ CASEWIT, KS COLWELL, WA GODDARD, and WM SKIFF. 1992. [Uff, a full periodic-table force-field for molecular mechanics and molecular-dynamics simulations](#). *JOURNAL OF THE AMERICAN CHEMICAL SOCIETY*, 114(25):10024–10035.
- [Rowe et al.(2020)Rowe, Deringer, Gasparotto, Csányi, and Michaelides] Patrick Rowe, Volker L. Deringer, Piero Gasparotto, Gábor Csányi, and Angelos Michaelides. 2020. [An accurate and transferable machine learning potential for carbon](#). *The Journal of Chemical Physics*, 153(3):034702.

- [Schütt et al.(2017)Schütt, Kindermans, Saucedo, Chmiela, Tkatchenko, and Müller] Kristof T. Schütt, Pieter-Jan Kindermans, Huziel E. Saucedo, Stefan Chmiela, Alexandre Tkatchenko, and Klaus-Robert Müller. 2017. [Schnet: A continuous-filter convolutional neural network for modeling quantum interactions.](#)
- [Scott et al.(1999)Scott, Hünenberger, Tironi, Mark, Billeter, Fennen, Torda, Huber, Krüger, and van Gunsteren] WRP Scott, PH Hünenberger, IG Tironi, AE Mark, SR Billeter, J Fennen, AE Torda, T Huber, P Krüger, and WF van Gunsteren. 1999. [The gromos biomolecular simulation program package.](#) *JOURNAL OF PHYSICAL CHEMISTRY A*, 103(19):3596–3607.
- [Smith et al.(2017)Smith, Isayev, and Roitberg] J. S. Smith, O. Isayev, and A. E. Roitberg. 2017. [Ani-1: an extensible neural network potential with dft accuracy at force field computational cost.](#) *Chem. Sci.*, 8:3192–3203.
- [Veličković et al.(2018)Veličković, Cucurull, Casanova, Romero, Liò, and Bengio] Petar Veličković, Guillem Cucurull, Arantxa Casanova, Adriana Romero, Pietro Liò, and Yoshua Bengio. 2018. [Graph attention networks.](#)
- [Vidal-Limon et al.(2022)Vidal-Limon, Aguilar-Toala, and Liceaga] Abraham Vidal-Limon, Jose E. Aguilar-Toala, and Andrea M. Liceaga. 2022. [Integration of molecular docking analysis and molecular dynamics simulations for studying food proteins and bioactive peptides.](#) *JOURNAL OF AGRICULTURAL AND FOOD CHEMISTRY*, 70(4):934–943.
- [Wang et al.(2021)Wang, Xu, Liu, Tang, and Geng] V. Wang, N. Xu, J.-C. Liu, G. Tang, and W.-T. Geng. 2021. [Vaspkit: A user-friendly interface facilitating high-throughput computing and analysis using vasp code.](#) *Computer Physics Communications*, 267:108033.
- [Wolpert(1992)] David H. Wolpert. 1992. [Stacked generalization.](#) *Neural Networks*, 5(2):241–259.
- [Xu et al.(2018)Xu, Li, Tian, Sonobe, ichi Kawarabayashi, and Jegelka] Keyulu Xu, Chengtao Li, Yonglong Tian, Tomohiro Sonobe, Ken ichi Kawarabayashi, and Stefanie Jegelka. 2018. [Representation learning on graphs with jumping knowledge networks.](#)
- [Zhang et al.(2018)Zhang, Han, Wang, Car, and E] Linfeng Zhang, Jiequn Han, Han Wang, Roberto Car, and Weinan E. 2018. [Deep potential molecular dynamics: A scalable model with the accuracy of quantum mechanics.](#) *Phys. Rev. Lett.*, 120:143001.
- [Zhang et al.(2019)Zhang, Lin, Wang, Car, and E] Linfeng Zhang, De-Ye Lin, Han Wang, Roberto Car, and Weinan E. 2019. [Active learning of uniformly accurate interatomic potentials for materials simulation.](#) *PHYSICAL REVIEW MATERIALS*, 3(2).
- [Zheng et al.(2019)Zheng, Chu, Zhao, Zhang, Guo, Wang, Jiang, and Zhao] Qijing Zheng, Weibin Chu, Chuanyu Zhao, Lili Zhang, Hongli Guo, Yanan Wang, Xiang Jiang, and Jin Zhao. 2019. [Ab initio nonadiabatic molecular dynamics investigations on the excited carriers in condensed matter systems.](#) *WIREs Computational Molecular Science*, 9(6):e1411.

## A Ablation Study

The ablation study, conducted on the ensemble comprising all 8 models for the methanol dataset as shown in Table 3, elucidated the pivotal role played by the ResNet component in the overall model performance. Moreover, a gradual degradation in performance was observed as the graph attention layers (GATs) were progressively removed from the architecture. These findings underscore the indispensable contributions of both the ResNet and the GAT layers to the model’s effectiveness, with the ResNet being crucial for achieving optimal results and the GATs substantially enhancing the model’s predictive capabilities.

Table 3: Performance of different architectures

Architecture	RMSE
Full (8 GAT + ResNet)	0.018
w/o ResNet	0.067
w/o 1 GAT and ResNet	0.0788
w/o 2 GAT and ResNet	0.0992
w/o 3 GAT and ResNet	0.1167
w/o 4 GAT and ResNet	0.1230
w/o 5 GAT and ResNet	0.1426

## B Data Distribution

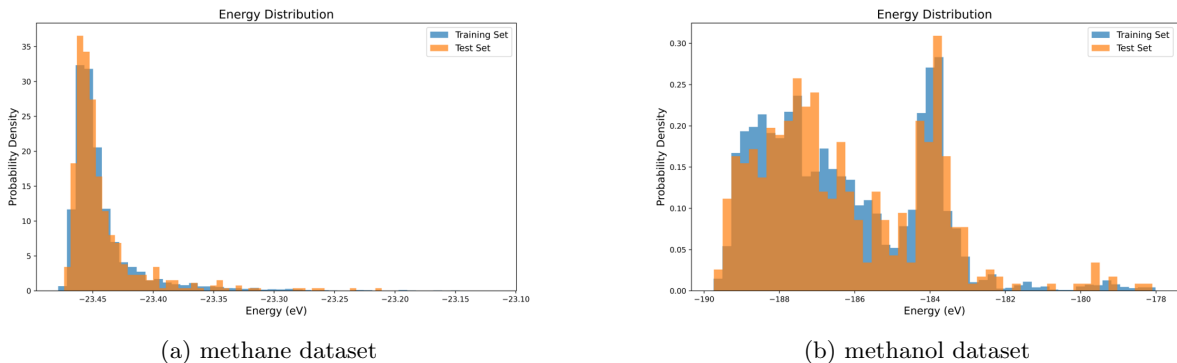


Figure 3: Energy distribution

To gain deeper insights into the nature of the datasets, we analyzed the energy distributions of the methane and methanol systems across the training and test sets. As illustrated in the figures, the methane dataset exhibits a relatively narrow energy distribution, while the methanol dataset displays a broader and more dispersed energy range. This discrepancy can be attributed to the increased complexity and higher degrees of freedom associated with the methanol molecule, leading to a more extensive configurational space.

It is noteworthy that for both methane and methanol, a high degree of consistency is observed between the energy distributions of the training and test sets, ensuring their statistical comparability. This consistency is crucial for evaluating the generalization capabilities of the trained models, as the test set should possess similar statistical properties to the training set to avoid issues such as overfitting or underfitting. Consequently, we can reasonably assert that the construction of these datasets is appropriate and provides a reliable foundation for model training and evaluation.

Through the analysis of the energy distributions, we not only unveil the inherent physicochemical differences between the methane and methanol systems but also validate the quality and reliability of the data. This lays a solid groundwork for subsequent model training and evaluation processes.

## C Training Setting Supplementary

The training parameters for all machine learning force fields can be found in our provided repository 3.2. As for the training of our models, we adopted an initial learning rate of  $1 \times 10^{-3}$  and a batch size of 256. We employed the cosine annealing learning rate schedule introduced in the SGDR (Stochastic Gradient Descent with Warm Restarts) algorithm [Loshchilov and Hutter(2016)]. This scheduler first linearly increases the learning rate from an initial value to a maximum value  $\eta_{\max}$  during a warmup period. After the warmup, the learning rate is then gradually decreased following a cosine curve, reaching a minimum value  $\eta_{\min}$  at the end of the total number of training epochs  $T_{\max}$ . Specifically, the learning rate  $\eta_t$  at epoch  $t$  is calculated as:

$$\eta_t = \eta_{\min} + \frac{1}{2}(\eta_{\max} - \eta_{\min}) \left( 1 + \cos \left( \frac{\pi t}{T_{\max}} \right) \right) \quad (8)$$

For the methane dataset, our models converged after training for 1500 epochs, while for the more complex methanol dataset, convergence was achieved after 300 epochs of training. The training was carried out on two NVIDIA Tesla V100-SXM2 GPUs.